CHAPTER 1

INTRODUCTION

1.1 General:

The use of wireless technology is advancing in almost every field. Along side with rapid technology advancement, IoT has become a protruding field providing interconnectivity among various devices from personal portable handsets to industrial automation. With increasing number of wireless devices demand higher data rates, low latency and energy efficient antenna systems. Therefore it became necessary to develop multiband antennas.

UWB antennas become very popular during early 2000's after FCC announced authorization for utilizing unlicensed frequency band from 3.1-10.6GHz with bandwidth of 7.5GHz and a fractional bandwidth of 110%. They are well-known for their low power consumption and deployed in data transmission and reception, location tracking and GPS services.

NB technology in IoT provides a wireless IoT protocol which uses Low-power wide area network (LPWAN). The provide some communication standards that allow devices to operate via cellular network either with GSM or LTE. Mainly NB antennas operate at frequencies 1.8GHz (GSM), 2.4GHz(WLAN) , 2.6GHz(LTE), 3.3GHz(5G).Some NB IoT applications include smart buildings, supply chain management, smart metering etc.

The proposed antenna architecture incorporates two Narrowband (NB) radiators, along with an Ultrawideband (UWB) radiator covering the frequency range of 3.1-10.6GHz. By strategically placing these radiators on the front side of an FRAME RADIATOR-4 (LOSSY FREE)loss-free substrate, with dimensions of 70x70x1.6mm³ and a relative permittivity of 4.4, the antenna system achieves comprehensive coverage of key IoT communication bands.

To mitigate mutual coupling and enhance reception efficiency, the NB radiators are orientated orthogonally to each other, while each element is equipped with a partial rectangular ground plane on the backside. This design approach ensures minimal interference between the individual radiators, thereby facilitating simultaneous operation and improving overall antenna performance.

One of the distinctive features of the proposed antenna is its ability to support multiple wireless standards concurrently, enabling seamless connectivity across diverse IoT ecosystems. Specifically, NB radiator-1 caters to GSM and WLAN frequencies, while NB radiator-2 is tailored for 5G communication, which aligns with the predominant frequency band for IoT devices. Furthermore, the real-time implementation of the proposed MIMO antenna validates its efficacy in practical scenarios, affirming its suitability for deployment in IoT applications where reliability, versatility, and spectral efficiency are paramount.

1.2 Overview of IoT Communication Technologies:

In the realm of IoT (Internet of Things) communication technologies, our project focusing on the Design of a Multiband MIMO Antenna for IoT applications holds significant relevance. IoT encompasses a vast array of interconnected devices and systems, necessitating diverse communication solutions to enable seamless data exchange and functionality.

Multiband MIMO Antenna design plays a crucial role in enabling robust and versatile communication capabilities for diverse IoT applications, accommodating various communication standards and frequency bands to meet the evolving demands of the IoT ecosystem.

Signal fading has traditionally been viewed as a problem with multipath propagation. Multiple-Input-Multiple-Output (MIMO) arrays, on the other hand, are now widely recognised as critical in wireless communication for increasing channel capacity, transmission speeds, and dependability. This is accomplished without the need of more frequency spectrum or higher transmission power. MIMO system developments are driven by diversity gain, spatial multiplexing, and interference reduction, which together drive performance improvements.

CHAPTER 2

LITERATURE SURVEY

It explores how wideband antennas are important for supporting a variety of IoT frequency bands and how MIMO systems can improve communication performance and reliability [1].The actualization of high-performance Internet of Things communication systems requires the integration of wideband and MIMO antenna technology. Compact planar structures were used to construct wideband MIMO antennas, resulting in a significant reduction in antenna size without sacrificing broad bandwidth and MIMO capabilities. Additionally, in order to increase flexibility and efficiency, created a reconfigurable MIMO antenna system that can adjust to various IoT frequency bands.

These studies demonstrate how wideband and MIMO antennas work well together for Internet of Things applications [1], A Compact planar MIMO antenna designed with Internet of Things applications in mind. In order to satisfy the needs of compact IoT devices, these studies emphasize how important it is for IoT antenna design to become more efficient and smaller. In addition, incorporating MIMO techniques has become a key tactic for improving the dependability and data throughput of Internet of Things networks. The continuous optimization of tiny planar MIMO antennas to meet the changing needs is the focus of future research efforts[2].

With the goal of achieving multi-band characteristics to satisfy the demands of contemporary communication systems, this work explores integrated patch antennas. In wireless communication, multi-band antennas are essential for meeting a variety of frequency needs. Related research have carefully examined performance variables like radiation pattern, bandwidth, and efficiency. By developing new methods for achieving multi-band functioning in small antenna designs, the research advances the area [3].

In order to shed light on fractal antenna architectures, this paper explores the construction and analysis of a sided fractal bow-tie dipole antenna. Previous studies have looked into using fractal shapes to improve the bandwidth and performance of antennas. The study emphasizes how

important fractal designs are to obtaining multi-band operation and compactness. Especially, the work provides new understandings of how to use Koch-like fractals to dipole antenna designs. The incorporation of fractal components into antenna design highlights how effective and efficient they can be [4].

The work tackles the urgent need for small and flexible antenna solutions by examining stub-loaded multi-band slotted rectangular microstrip antennas. It is emphasized how important multi-band antennas are to modern wireless communication systems that are designed to meet a variety of frequency requirements. Especially noteworthy is the research's original insights into combining slots and stubs to improve antenna performance in a variety of frequency bands. Subsequent research paths may focus on more antenna optimization for a wide range of applications, including wireless networking, satellite communication, and the Internet of Things [5].

The goal of this novel antenna design is to outperform conventional designs in terms of broadband performance. Through dual-band operation, the antenna makes use of the special qualities of modified Sierpinski fractals, enabling simultaneous transmission or reception across two different frequency bands. The study demonstrates how fractal shapes can increase antenna efficiency and bandwidth. The project shows the performance benefits and practical viability of using modified Sierpinski fractals in dielectric resonator antennas through experimental validation. This work provides important new information about how to use fractal geometry to improve broadband antenna designs [6].

In order to provide triple-band operation for WLAN and WiMAX communication standards, this project makes use of Finite Difference Time Domain (FDTD) techniques. Motivated by the concepts of metamaterials, the antenna design efficiently manipulates electromagnetic waves. FDTD research and simulation show that the antenna performs better throughout a range of frequency bands [7].

To enable dual-band operation, the antenna design has slots that are thoughtfully positioned on a triangular monopole construction. The antenna can function effectively in two different frequency bands that are important to RFID systems thanks to its creative configuration. The project verifies

the antenna's ability to achieve compact dimensions without sacrificing performance through analysis and experimentation [8].

In order to facilitate circular polarization and broadband operation, this study offers a cross-shaped planar monopole antenna with a ground plane extension. The antenna maintains performance while being small thanks to careful element placement. Its efficacy in offering circular polarization and wide frequency coverage is validated experimentally [9].

In order to accomplish dual-band functioning, the antenna design takes advantage of the special qualities of half-mode substrate integrated cavity structures. The antenna's ability to function across two frequency bands is verified through experiments, providing possible uses in a range of wireless communication systems [10].

The antenna design meets the various frequency needs of Internet of Things devices by achieving ultrawideband characteristics through the use of printed construction and CPW feeding [11].

CHAPTER 3

PROPOSED SYSTEM

3.1 System Design: System design flow is detailed below

3.2 Software Requirements:

- CST Studio Suite Software

3.3 Hardware Requirements:

- Six port MIM Antenna
- FRAME RADIATOR-4 (LOSSY FREE) Substrate
- 3.GSM Module
- 4.LDR Sensor
- 5.Microcontroller

3.4 Block Diagram:

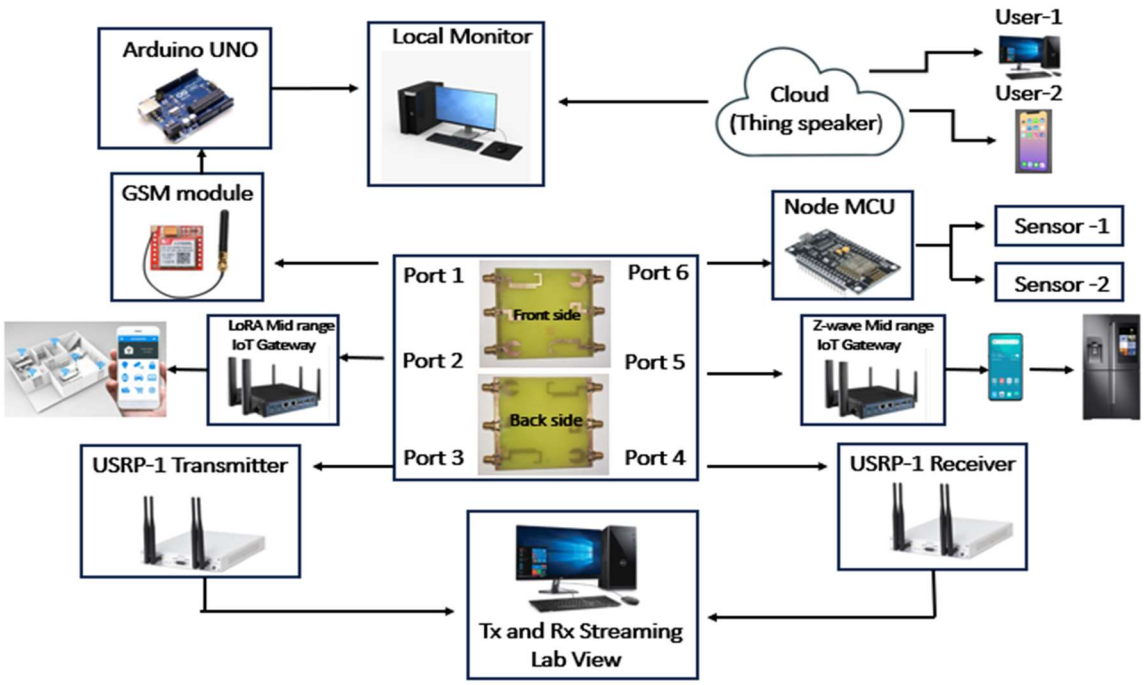

Figure 3.1 Block diagram of smart home IoT Applications Using Proposed Antenna

3.5 DESIGN FLOW PROCESS:

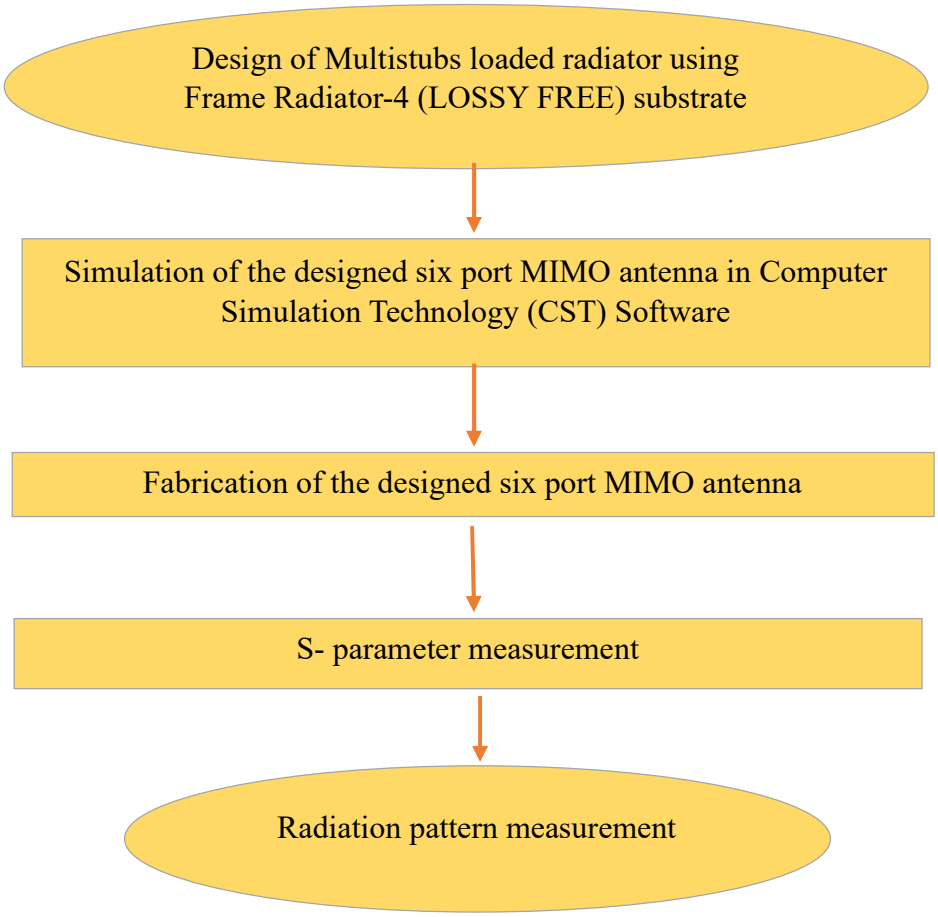

Figure 3.2: Flow diagram of MIMO Implementation

Designing a six port MIMO antenna with multi stub loading on a FRAME RADIATOR-4 (LOSSY FREE) substrate involves several key steps. First, the frequency bands for operation need to be determined, typically spanning GSM, LTE, and Wi-Fi frequencies. FRAME RADIATOR-4 (LOSSY FREE) substrate, known for its common usage and cost-effectiveness, is chosen, considering its dielectric constant and thickness.

Next, dimensions are calculated based on transmission line theory. These calculations aid in designing the main radiator, typically a patch antenna, for the lowest frequency band. Additional stubs are then introduced strategically to achieve resonance in the other frequency bands. These stubs' lengths and positions are calculated meticulously to target the desired frequencies accurately.

The design is then simulated using CST software. Substrate properties like dielectric constant and thickness are input, and the antenna's geometry, including the main radiator and stubs, is modeled. Suitable boundary conditions are assigned, and a frequency sweep covering the desired bands is set up. The simulation results, encompassing return loss, impedance bandwidth, and radiation patterns, are analyzed for optimization.

Once the simulation results are satisfactory, fabrication of the antenna begins. The design is transferred to a fabrication layout, and suitable materials, such as copper and FRAME RADIATOR-4 (LOSSY FREE)for the substrate, are chosen.

After fabrication, the antenna's performance is verified through S-parameter measurement. Using a network analyzer, the antenna's S-parameters are measured over the desired frequency range, and the results are analyzed to confirm its performance.

Finally, radiation pattern measurements are conducted. The fabricated antenna is mounted in a test environment, and radiation patterns are measured in both E-plane and H-plane across the desired frequency bands. These measurements are analyzed to ensure that the antenna meets design specifications for gain, beanwidth and sidelobe levels.

3.6 ENGINEERING STANDARDS:

- Federal communications commission (FCC)
- IEEE-802.11-WiFi, IEEE 802.15.4 MAC PAN, IEEE 802.11 IoT
- SDR-IEEE

3.7 MULTIDISCIPLINARY ASPECTS:

IoT Applications: Understanding the specific requirements and constraints of IoT applications, such as sensor data transmission, energy efficiency, and network scalability, guides the design process to meet application-specific needs.

Interdisciplinary Collaboration: Collaboration between experts in different fields, including electrical engineering, computer science, telecommunications, and material science, is essential to address the diverse challenges and optimize the design of the multiband MIMO antenna for IoT applications.

CHAPTER-4

ANTENNA DESIGN

4.1 Antenna Design:

The below design process illustrates the antenna design in Software for desired operating frequency.

4.1.1 NB-1 ANTENNA (Radiator-1):

The radiator-1 comprises a antenna height of λ/4 and a partial rectangular ground plane at the back of substrate. The total length (H) of radiator which has a max operating frequency (fr) is determined using formula

$$f_{Ri} = \frac{c}{4Ls_j\sqrt{\varepsilon_e}}$$

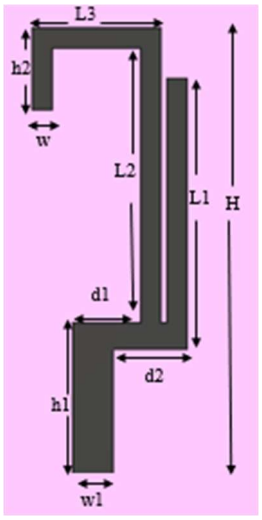

Figure 4.1: Development of designed Narrowband element

The design entails a Multiband MIMO antenna featuring one narrow band with a centered at 1.8 GHz and 2.4 GHz. This antenna is constructed on an FRAME RADIATOR-4 (LOSSY FREE) substrate. It's engineered to facilitate efficient communication across multiple frequency ranges simultaneously. By leveraging the specific frequencies of 1.8 GHz and 2.4 GHz, it enables robust connectivity suitable for diverse applications. The FRAME RADIATOR-4 (LOSSY FREE)

substrate provides a stable and cost-effective foundation for the antenna's operation, making it conducive for various wireless communication systems. This design represents an innovative solution catering to the growing demand for multiband antennas in modern communication networks.

Table 4.1: Dimensions of proposed NB-1 antenna

Parameter	Dimension(mm)	Parameter	Dimension(mm)
H	32.5	W1	3
H1	11	W2	1.5
H2	6	d1	3.5
L1	19	d2	5.5
L3	8		

The NB-1 antenna design demonstrates resonance at center frequencies of 1.8 GHz and 2.4 GHz, as depicted in the provided figure. Visual inspection reveals that the S11 parameter remains below -10 dB throughout the operating bandwidth.

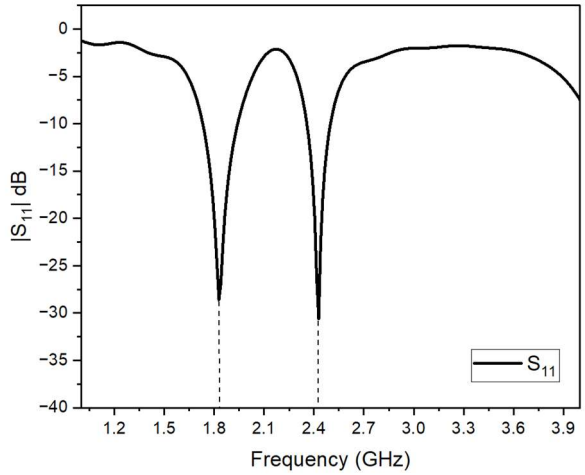

Figure 4.2: S11 of the proposed unit cell

A comparison between the simulated and tested results shows a slight deviation from the center frequency, which depends on various factors after fabrication. The theoretical operating frequency of the antenna is 1.8GHz and 2.4GHz, which are obtained accurately in simulation. However, when tested, the response is shifted by approximately 0.2GHz, resulting in 1.7GHz and 2.2GHz, respectively. Although the response is less than -10dB at 2.2GHz, it is still considered satisfactory.

4.1.2 NB-2 Antenna (Radiator-2):

Similar to radiator-1, the inverted 7 shaped antenna is also an NB antenna used for 5g IOT devices application with an operating frequency of 3.3GHz. the length of radiator is also calculated using the above formula. The simulation result of antenna is shown below. The stubs are of sizes L1, L2, h2, L3 are mentioned in below given table.

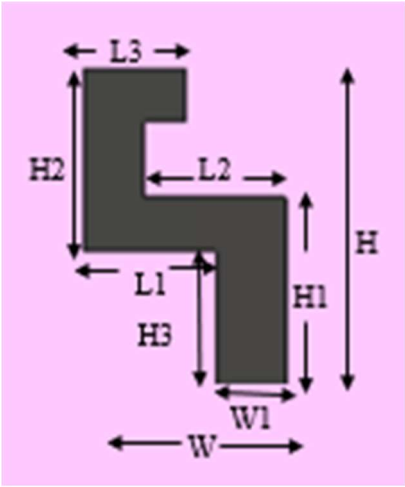

Figure 4.3: Development of designed NB element

The design aims to develop a Multiband MIMO antenna featuring a single narrow band focused at 3.3 GHz, positioned on an FR4 substrate. Its primary objective is to enhance communication effectiveness within a designated frequency range, fostering reliable connectivity across diverse applications. Leveraging the FR4 substrate ensures stability and cost-efficiency in the antenna's performance, rendering it applicable for deployment across a spectrum of wireless communication systems. This design embodies an inventive solution meeting the growing need for multiband antennas in contemporary communication networks.

Table 4.2: Dimensions of proposed NB-2 antenna

Parameter	Dimension(mm)	Parameter	Dimension(mm)	Parameter	Dimension(mm)
H	21	H3	4	L3	3
H1	7	L1	5.5		
H2	11	L2	3.5		

The NB-2 antenna design demonstrates resonance at center frequencies of 3.3Ghz, as depicted in the provided figure. Visual inspection reveals that the S11 parameter remains below -10 dB throughout the operating bandwidth. The simulation results of reflection coefficient of antenna is 3.3GHz which is equal to calculated theoretical value

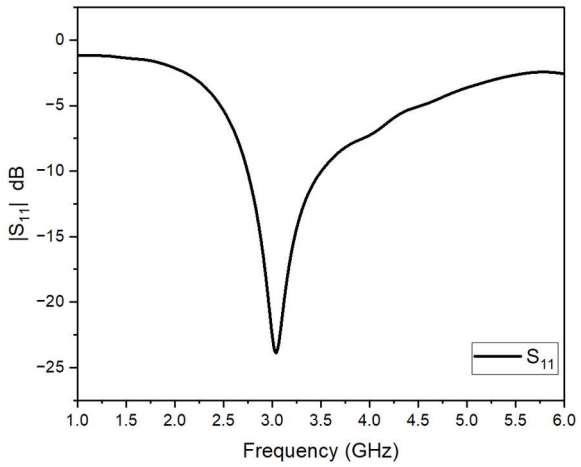

Figure 4.4: S11 of the proposed unit cell

The graph in the figure 4.4 compares the simulated and tested results, with all other ports being isolated during the measurements. A close examination of the graph reveals that the simulated and measured data exhibit a strong overall correspondence. The antenna's simulated frequency is approximately 3.3 GHz, while the tested frequency is around 3 GHz. The slight variation in the frequency of the sharp curve may be attributed to internal or external factors.

4.1.3 Design of UWB ANTENNA :

A circular radiator with slotted rectangular portion is designed for UWB application. A circle of radius 8mm is placed over a rectangular feed line having dimensions 7 x 3.5mm^2 This shaped antenna operated over a resonating frequency of 2-11GHz range with isolation nearly 10dB. To improve the value a rectangular slot with dimension 10 x 3.5 mm^2 is attenuated. Now the designed UWB antenna radiates over a frequency of 3-11GHz with an isolation of <15dB.

The total height of antenna is of λ/4 of the wavelength. Then the whole radiator pieces are intersected into one object.

The starting frequency of antenna is calculated by the formula

$$F = \frac{c}{\lambda} = \frac{7 \cdot 2}{L+r+p} \text{ GHz} \quad \text{.....(1)}$$

Where p is length of 50Ω feedline in cm.

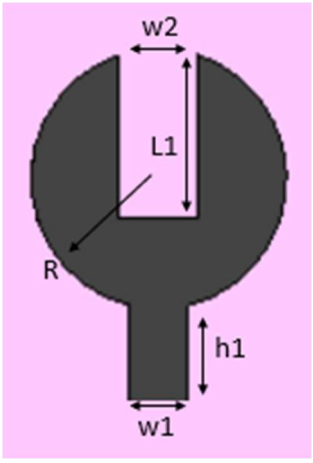

Figure 4.5: Designed UWB element

The UWB antenna design demonstrates resonance at a frequency range of 3.3-10.6Ghz as depicted in the provided figure. Visual inspection reveals that the S11 parameter remains below -10 dB throughout the operating bandwidth.

Table 4.3: Dimensions of proposed UWB antenna

Parameters	Dimensions	Parameters	Dimensions
L1	8	h1	6.1
W2	4	G	3.5
r	9.5	W	2
W1	5		

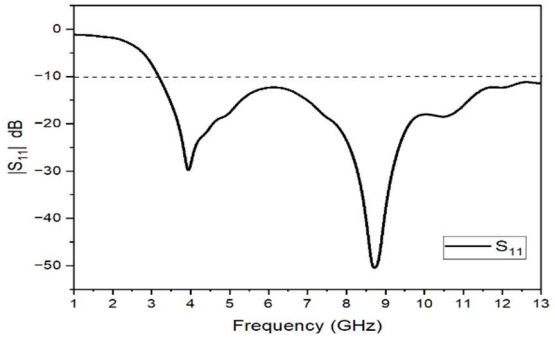

Figure 4.6: Simulation result of designed UWB antenna

In Figure 4.6, the comparison between simulated and tested results is presented, with all other ports isolated during measurements. Upon thorough examination of the graph, it becomes apparent that the simulated and measured data align closely overall. The simulated frequency range for the antenna spans from 3.3 to 10.6 GHz. Any slight deviation in the frequency of the sharp curve could potentially be attributed to internal or external factors influencing the measurements.

4.1.4 Surface current Distribution

Surface current distribution in antenna illustrates how electric currents are distributed across the antenna's surface, impacting its radiation characteristics and interaction between antenna elements. Understanding this distribution is crucial for optimizing antenna performance in terms of efficiency and radiation pattern control, especially in densely packed MIMO systems where mutual coupling can significantly affect overall performance. The surface current distribution of the designed antenna is simulated at 1.8Ghz,2.4Ghz,3.3Ghz is excited as depiction from the figure 4.11-4.13.

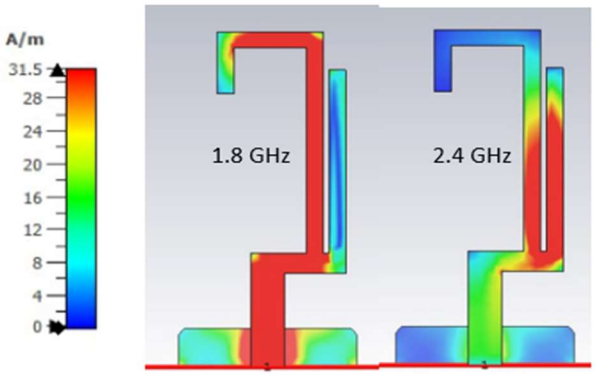

Figure 4.7: Simulated electric field distribution of NB antenna at 1.8GHz (a) and 2.4GHz(b).

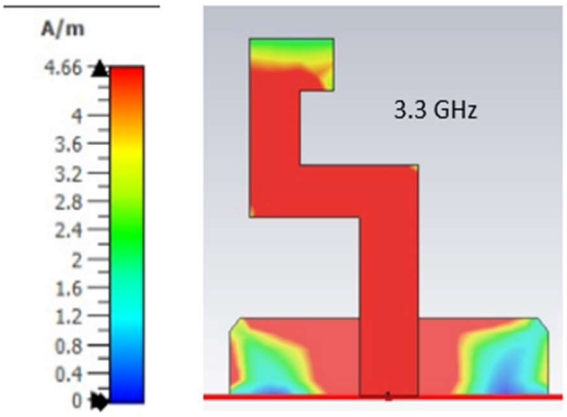

Figure 4.8: Surface current distributon of NB antenna which has a operating frequency of 3.3GHz.

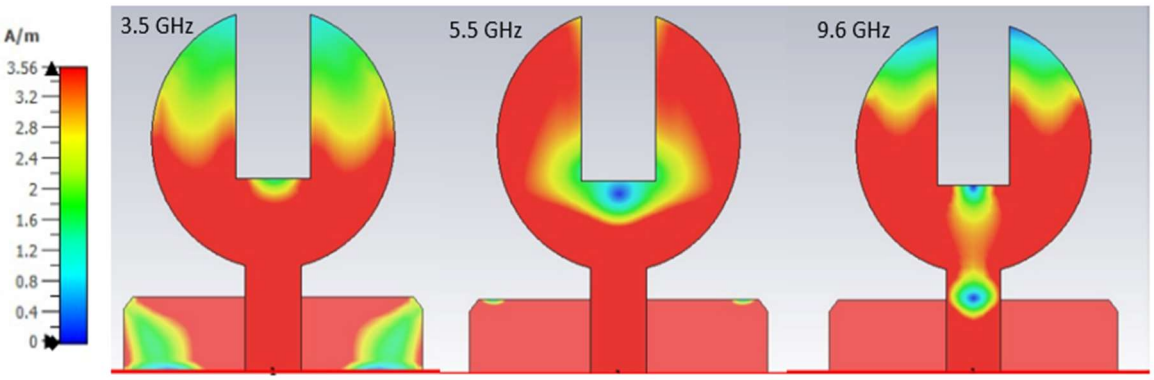

Figure 4.9: Surface current distribution of UWB antenna at (a) 3.5GHz, (b) 5.5GHz, (c) 9.6GHz

4.1.5 MIMO Implementation

A unique six-element MIMO antenna arrangement combines two narrowband (UWB) and one ultrawideband (NB) elements on a same ground plane. This configuration, which uses a Frame Radiator-4 substrate, maximises versatility by combining UWB's wide frequency coverage with NB's concentrated bands. The 70mm x 70mm x 1.6mm shape allows for high-speed data transmission, making it excellent for 5G and a variety of other applications. Careful positioning reduces inter-element interaction.

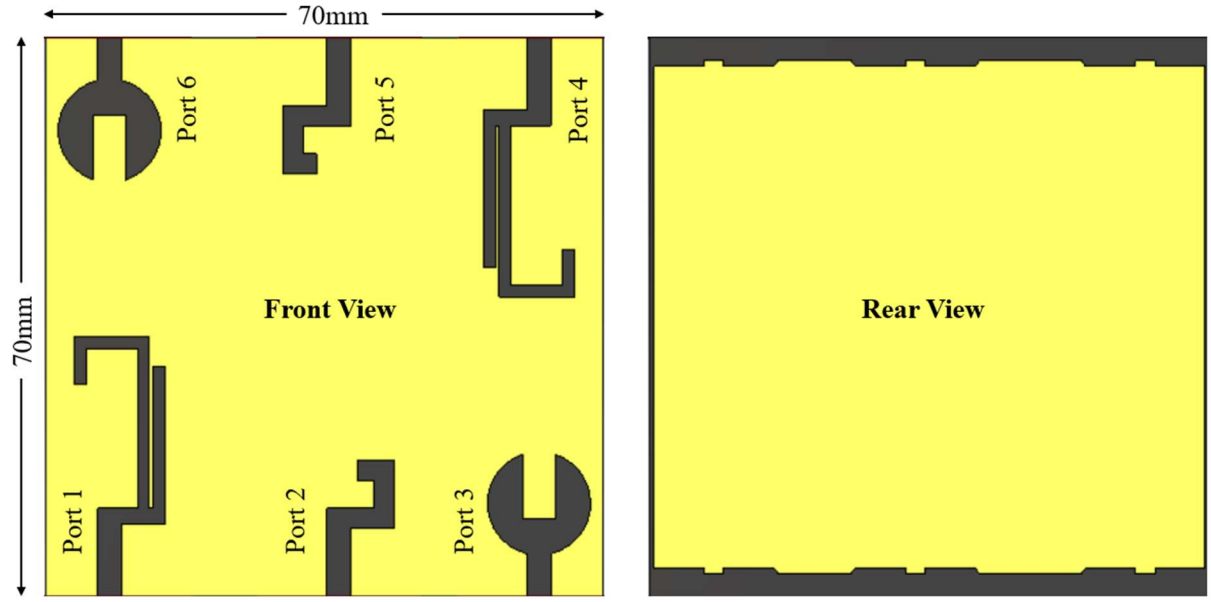

(a) (b)

Figure 4.10: (a) Front view and (b) back view of MIMO Antenna

Before the fabrication process, the dimensions and design constraints of the antenna are meticulously optimized using CST software, ensuring accurate results for real-time operation. All the radiators are evenly spaced horizontally. The obtained data from the prototype closely matches the simulated results, while slight differences may occur due to fabrication flaws, connector losses, material impurities, and measurement nuances.

CHAPTER 5

RESULTS & DISCUSSION

5.1 S-Parameter:

This section provides comprehensive details on the S-parameters, radiation pattern, gain, and total efficiency of the designed antenna. It encompasses MIMO parametric analysis and real-time validation. The fabricated 4-port UWB MIMO antenna, utilizing an FR4 substrate, is presented, along with the measured S-parameter data obtained using a VNA (vector network analyzer) setup, as depicted in Figure 5.1. Furthermore, Antenna can be effectively used in MIMO systems to improve the system performance and radiate signals in a way that minimizes the amount of signal coupling between them. Therefore, the designed antenna is in accordance with simulated and measured result.

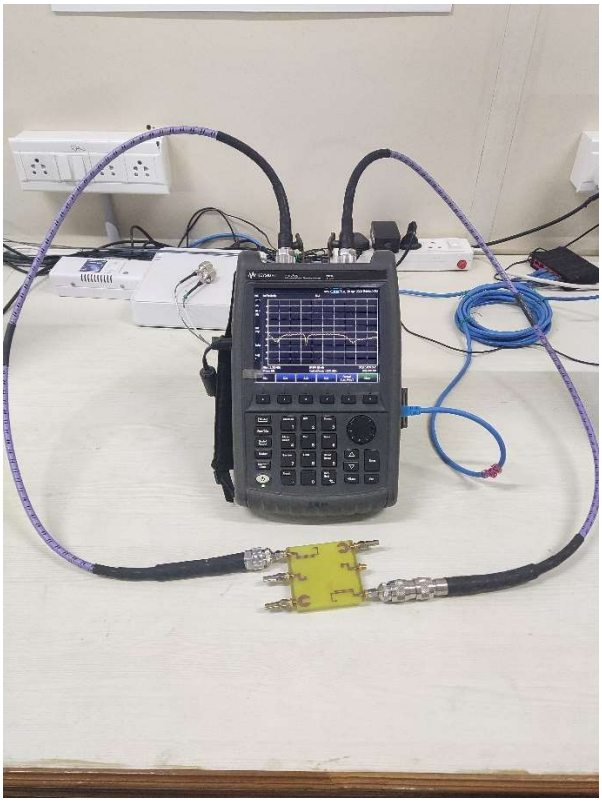

Figure 5.1: Vector Network Analyzer setup of designed MIMO Antenna

The below figure 5.2 shows the response narrow band radiator with other radiators which is apparent and desired. The response is below 15dB which makes its response accurate when fabricated.

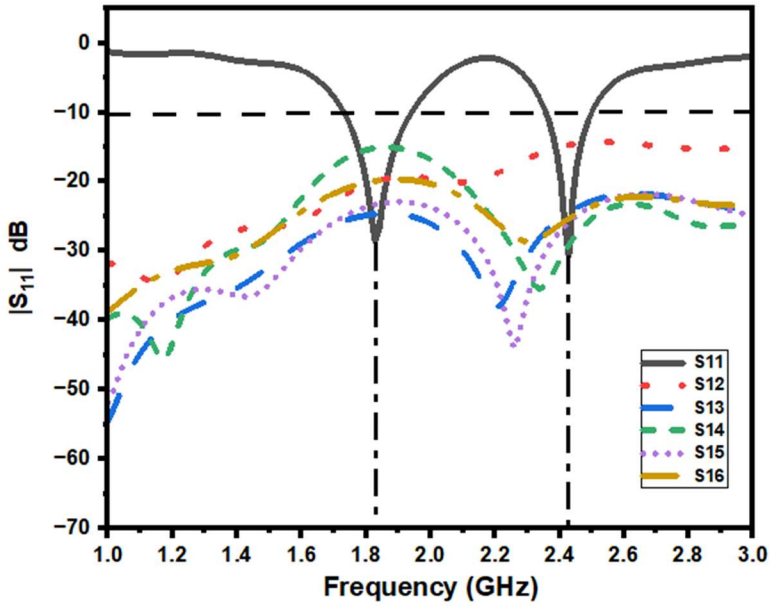

Figure 5.2: Measured S-Parameter set of proposed integrated NB-1 MIMO antenna

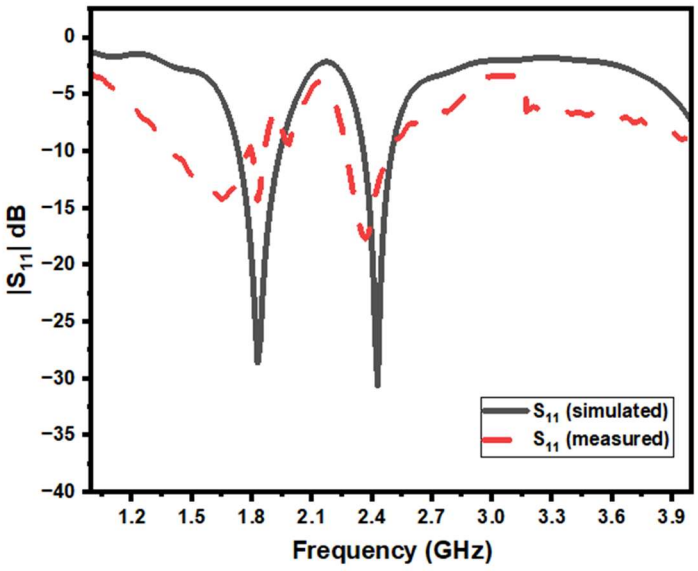

Figure 5.3: S11 of proposed NB antenna

The below figure 5.14 shows the simulated results of 5g radiator which has good symmetry with other elements. The 5g radiator is place between NB and UWB elements. This shows a good response at 3.3GHz which is desired frequency when simulated. The mutual coupling between each element is below -20dB when simulated which can be around -10dB when fabricated.

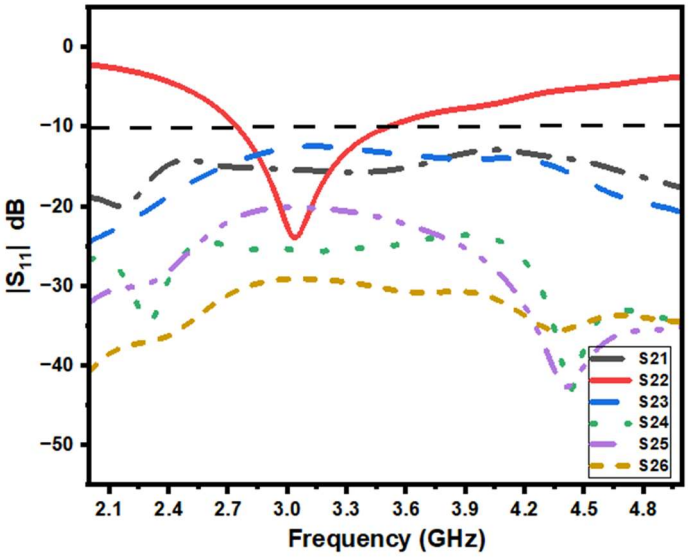

Figure 5.4: Measured reflection coefficients and mutual coupling of integrated NB-2 MIMO antenna

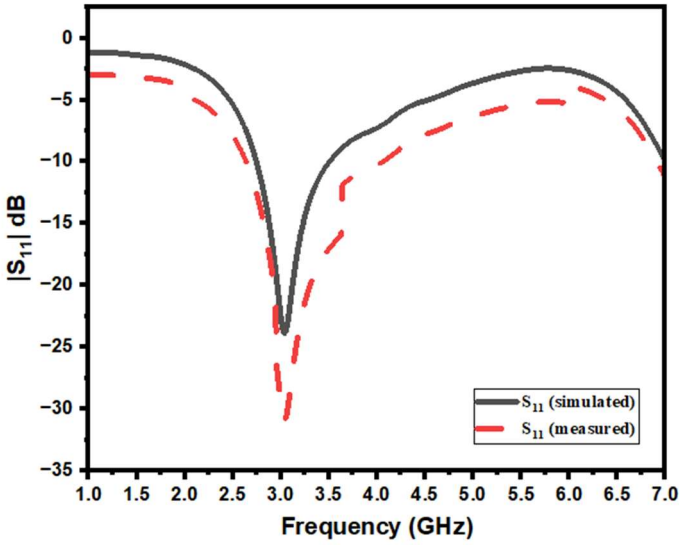

Figure 5.5: S11 of NB-2 antenna

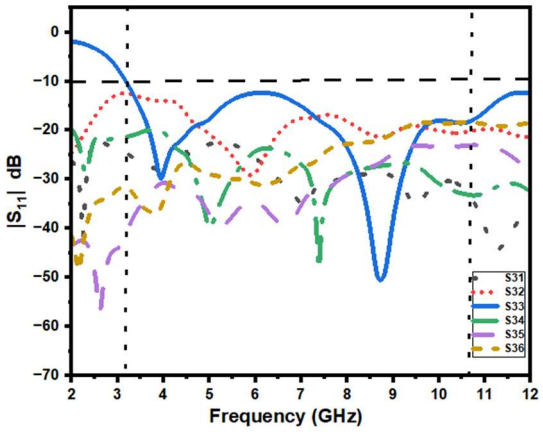

Figure 5.6: Measured S-Parameter set of proposed integrated UWB MIMO antenna

The UWB element simulation results is shown above fig 5.16 which has an operating frequency between 3.1-10.5 GHz. The response is below -15dB during the entire operating range. Apart from mutual coupling it also provides good response to other elements which makes the entire MIMO system to respond for various applications at a time.

5.2 Gain and Total Efficiency

The far-field gain and overall efficiency of the designed MIMO antenna at port 1 are illustrated Figure 5.21

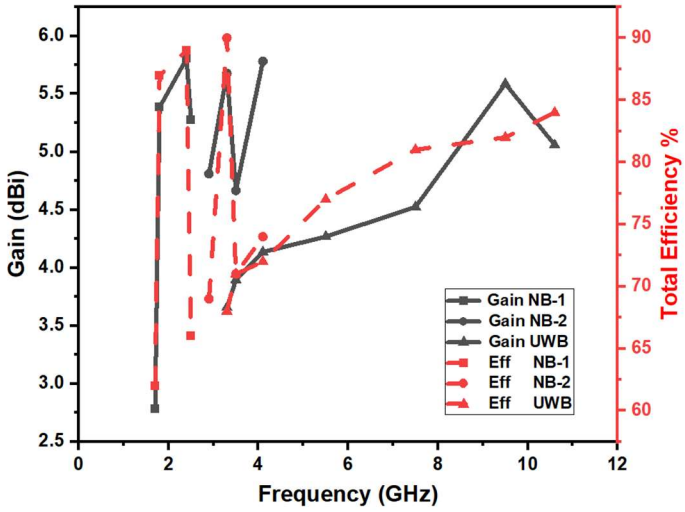

Fig 5.7: Gain and Efficiency Of Proposed MIMIO Antenna

5.3 Radiation Pattern:

The radiation patterns of a 6-port MIMO antenna were measured in an anechoic chamber, showing the co-polarization and cross-polarization radiation patterns in the E-plane (X-Z) and H-plane (Y-Z) at narrowband frequencies of 1.8, 2.4, and 3.3 GHz and wideband frequencies of 3.5, 5.5, 8.5, and 10.4 GHz.

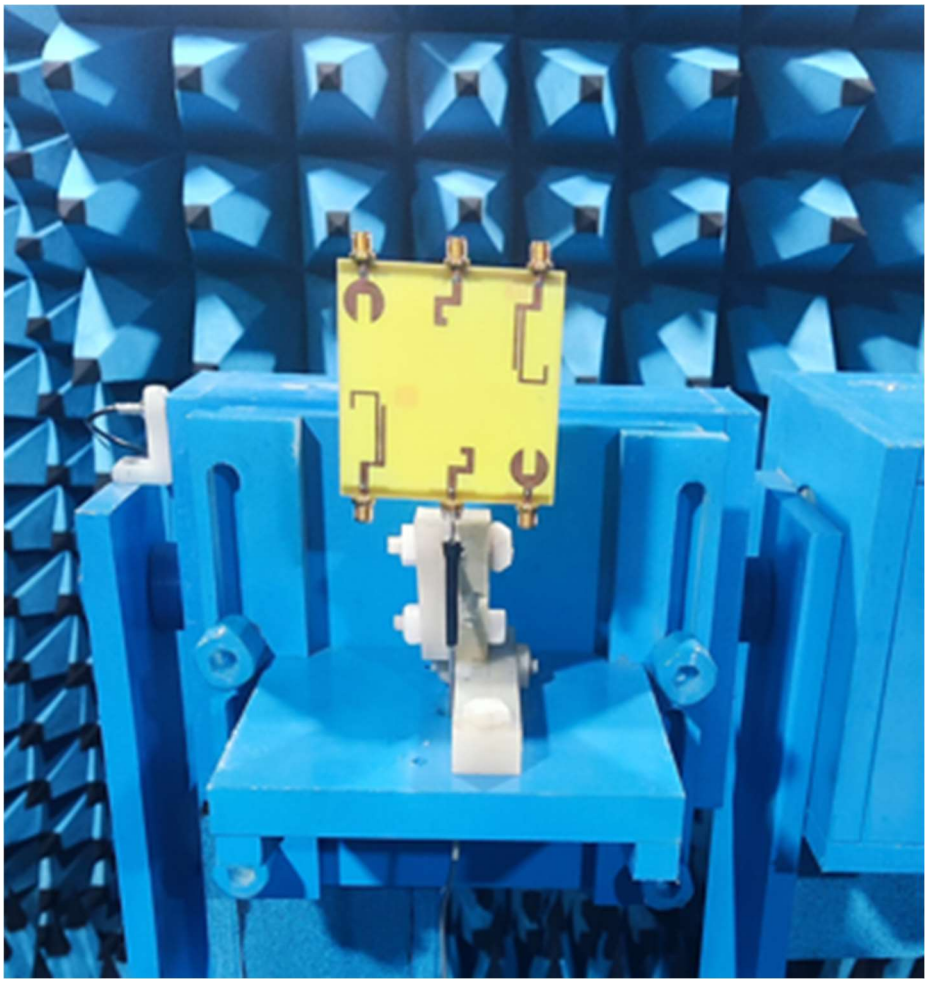

Figure 5.8: The designed antenna unit under test in anechoic chamber

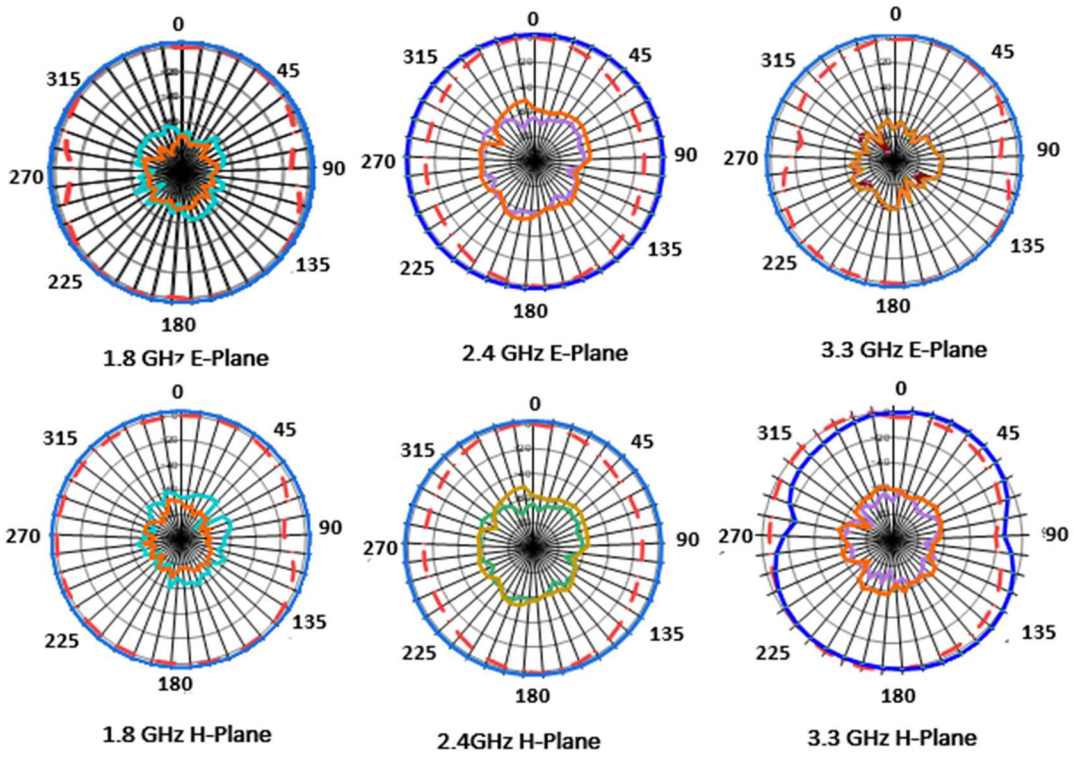

Figure 5.9: Radiation pattern of NB antenna

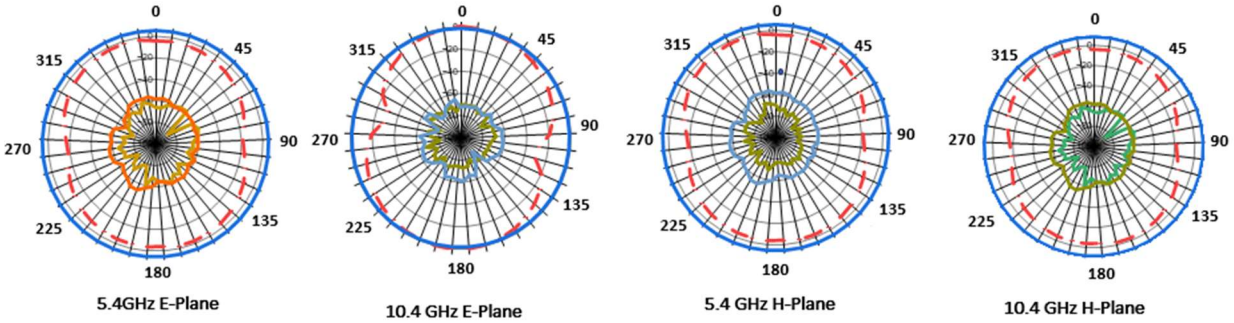

Figure 5.10: Radiation pattern of proposed UWB antena

5.4 Envelope Correlation Coefficient:

The Envelope Correlation Coefficient (ECC) serves as an indicator of the correlation among the signal amplitudes received by individual antennas within a MIMO system, reflecting the similarity or dissimilarity in their amplitudes. In practical MIMO systems, a low ECC is preferred, as it signifies uncorrelated signals received by antennas, enhancing system diversity and minimizing interference. Conversely, a high ECC can degrade performance and increase susceptibility to interference. Notably, the suggested antenna system's measured ECC. A theoretical ECC of 0 is ideal, but for real-world implementation, an ECC value of less than 0.5 is desirable. The formula for calculating ECC from the far field is provided below. The far field-based ECC of the antenna can be calculated based on Equation (1)

$$\rho e = \frac{|s_{11}s_{12}+s_{21}s_{22}|^2}{(1-|S11|^2-|S21|^2)(1-|S22|^2-|S12|^2)} \quad \text{.....(2)}$$

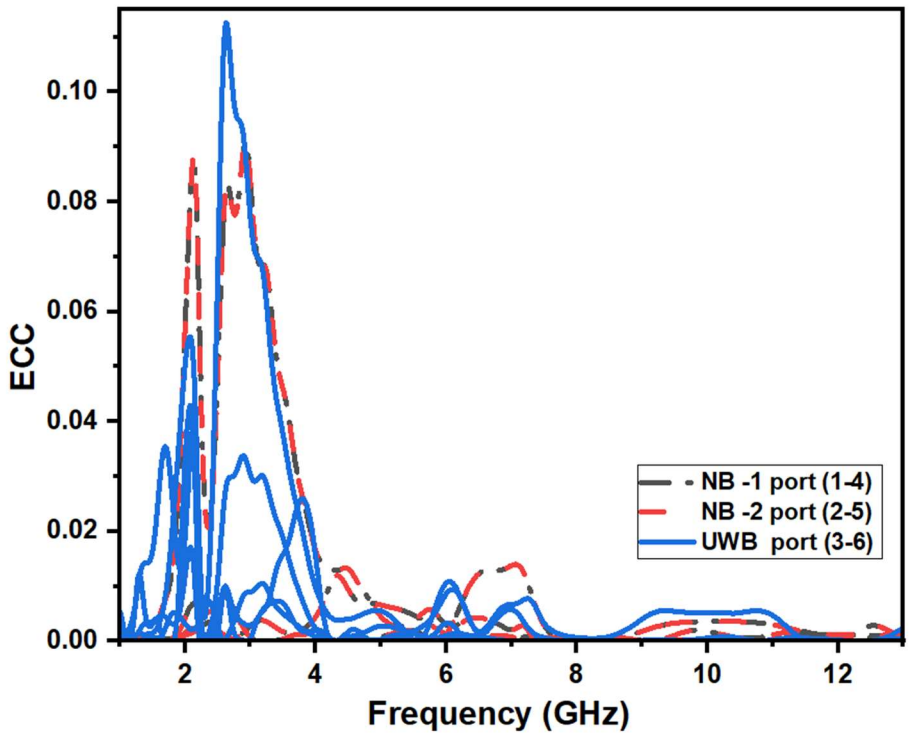

Figure 5.11: ECC of Proposed MIMO Antenna

The figure 5.41 demonstrates the measured ECC value of the suggested antenna system. It was observed from the graph that the ECC remains below 0.004 throughout the operating bandwidth of 1.8Ghz,2.4Ghz,3.3Ghz,3.5-10.6Ghz.

5.5 Diversity Gain:

The Diversity Gain (DG) in a MIMO antenna system denotes the improvement in signal quality or performance derived from employing several antennas for transmission and reception of signal. Generally, a system equipped with multiple antennas can attain superior diversity gain in comparison to a single-antenna system. This advantage arises from the ability of the former to leverage signal variations, thereby bolstering overall signal strength. Calculation of the antenna's diversity gain can be performed utilizing Equation (2).

$$DG = 10\sqrt{1 - ECC^2} \quad \text{.....(3)}$$

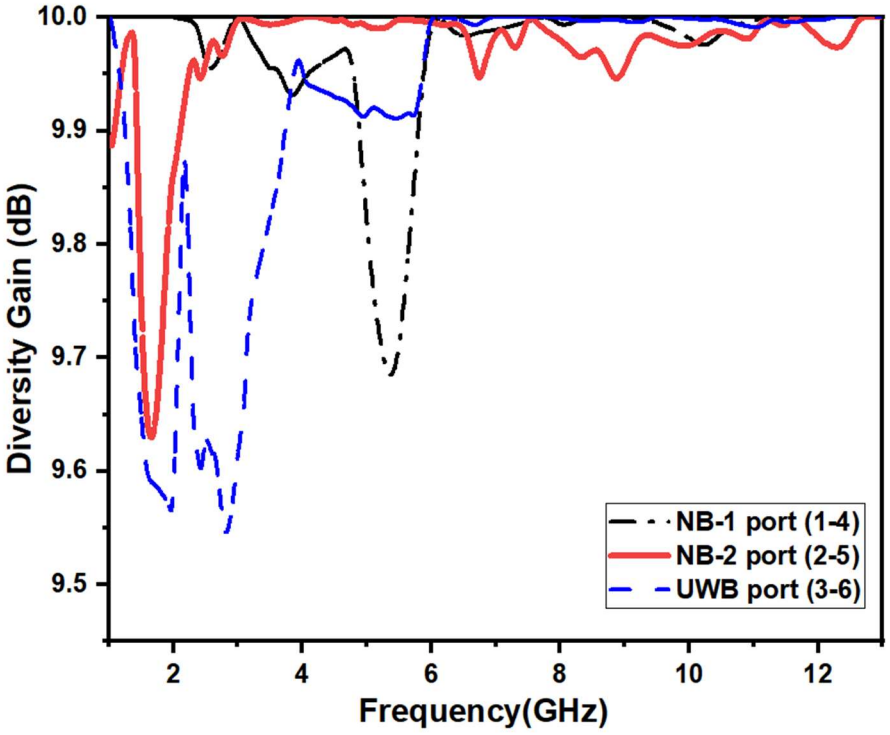

Figure 5.12: Diversity Gain of Proposed MIMO Antenna

Illustrated in the figure 5.51 that the designed 6-port MIMO antenna diversity gain. It can be noted that DG is >9.98 at the entire operating bandwidth.

5.6 Total Active Reflection Coefficient:

The Total Active Reflection Coefficient (TARC) serves as an indicator of the MIMO antenna system's efficacy in transmitting and receiving signals. Within a MIMO setup, signals from each antenna may interfere with one another, resulting in diminished signal quality and performance. TARC quantifies the extent of interference among the antennas. It is a critical element in determining the mutual coupling between multiple radiators in MIMO antenna systems. The equation for calculating TARC for a six-port antenna is provided below. The variable θ ranges from 0 to 2π.It can be calculated by using the equation (3)

$$\text{TARC} = \sqrt{\frac{(S_{11}+S_{12}e^{j\theta})^2+(S_{21}+S_{22}e^{j\theta})^2}{2}} \quad \text{.....(4)}$$

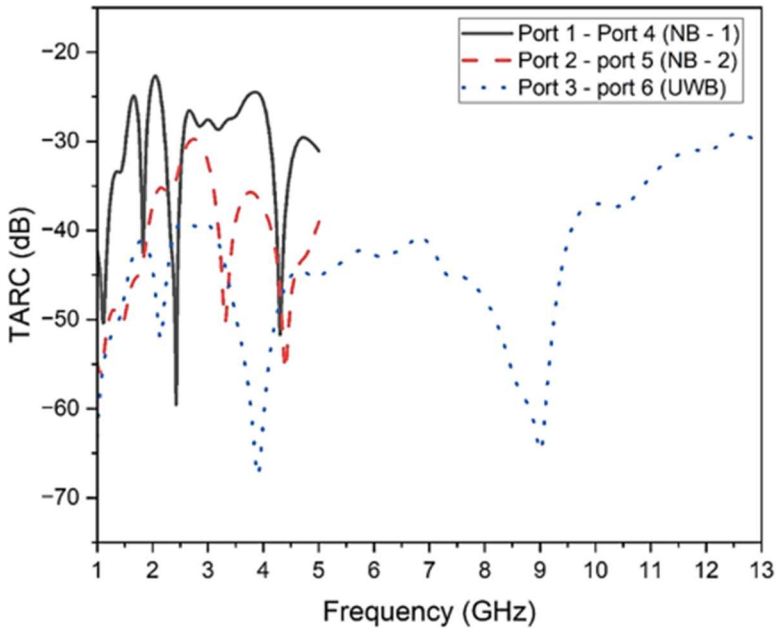

Figure 5.13: TARC of Proposed MIMO antenna

5.7 Channel Capacity Loss:

In MIMO systems, achieving a low CCL (Channel Capacity Loss) is paramount, ideally approaching zero, to signify minimal loss in channel capacity. A reduced CCL enables the MIMO system to leverage multiple antennas effectively, mitigating fading, interference, and noise effects, thereby enhancing the overall quality of the communication system. The Channel Capacity Loss (CCL) is characterized as the maximum distance over which communication takes place without experiencing possible loss during transmission. The acceptable range of must be less than 0.4 bits/sec/Hz.It can be Calculated by using the equation (4).

$$CCL = -\log_2 |\psi R| \quad \ldots\ldots\ldots\ldots\ldots(5)$$

$$\psi R = \begin{bmatrix} \emptyset^{11} & \emptyset^{12} \\ \emptyset^{21} & \emptyset^{22} \end{bmatrix}$$

Where ψ^R is the receiving antenna correlation.

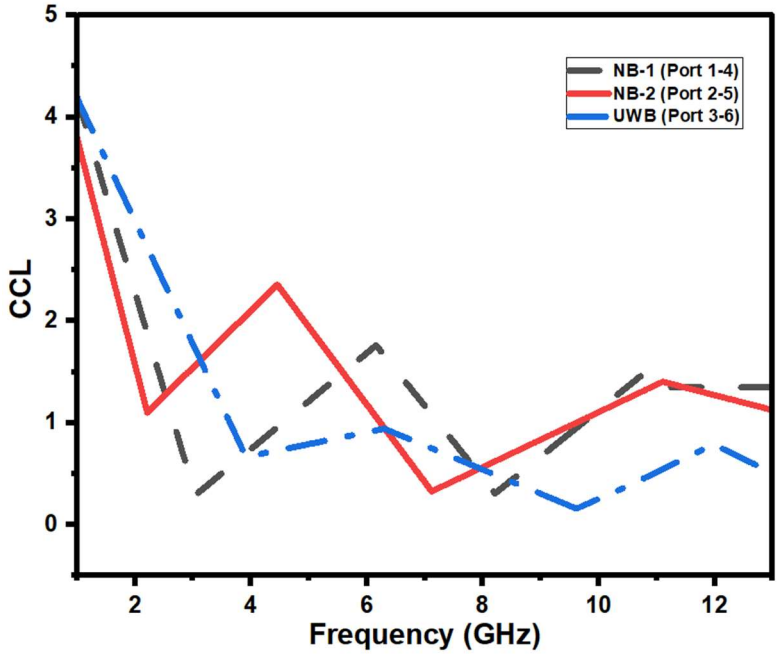

Figure 5.14: CCL of proposed MIMO antenna

5.8 Mean Effective Gain:

The Mean Effective Gain (MEG) is an important statistic for evaluating the performance of MIMO antennas. It represents an antenna's average gain in all available directions, taking into account both the radiation pattern and the spatial correlation of its many parts.

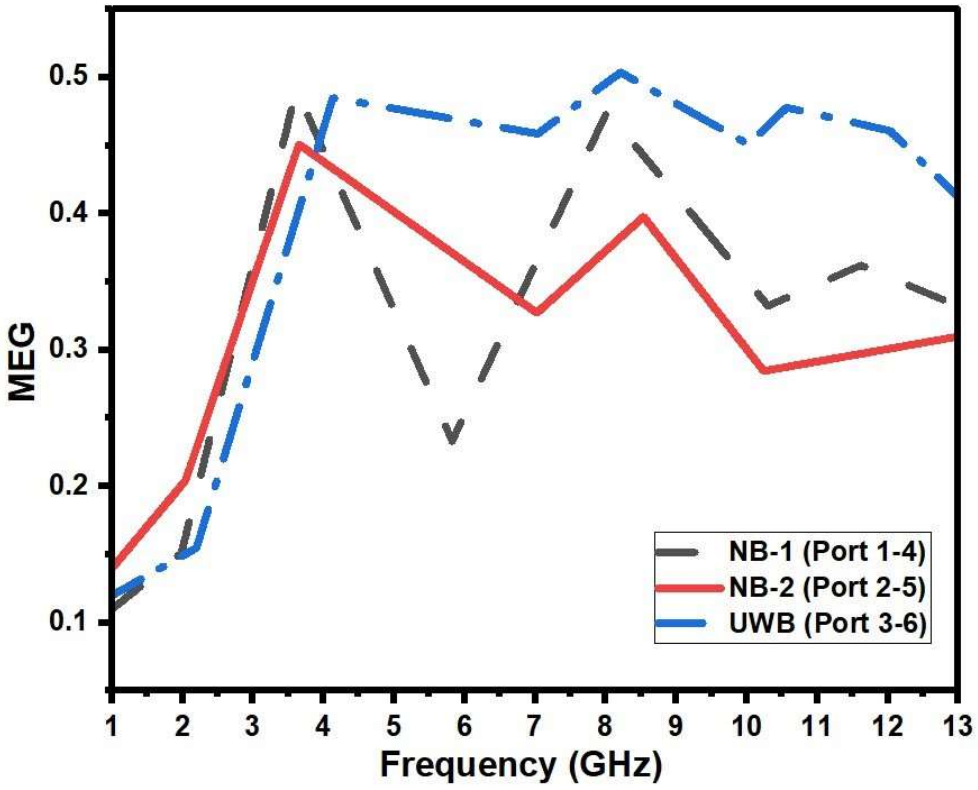

Figure 5.15: MEG of proposed MIMO Antenna

Table 5.1: Performance summary of preferred MIMO antenna

Parameter	Value
Mutual Coupling (MC)	**< -15dB**
Diversity gain (DG)	**Nearly 10**
Mean effective gain	**3 < MEG (dB) < -12**
Channel Capacity Loss	**< 0.4 bits/Hz/Sec**
Envelope Correlation Coefficient (ECC)	**< 0.5**
Total Active Reflection Coefficient (TARC)	**< 0dB**

5.9 DESIGN EQUATIONS:

- $\boldsymbol{F = \frac{c}{\lambda} = \frac{7 \cdot 2}{L+r+p}}$ **GHz ……(1)**
- $\boldsymbol{\rho e = \frac{|s_{11}s_{12}+s_{21}s_{22}|^2}{(1-|S11|^2-|S21|^2)(1-|S22|^2-|S12|^2)}}$ **……(2)**
- $\boldsymbol{DG = 10\sqrt{1-ECC^2}}$ **……(3)**
- $\textbf{TARC} = \sqrt{\frac{\left(S_{11}+S_{12}e^{j\theta}\right)^2+\left(S_{21}+S_{22}e^{j\theta}\right)^2}{2}}$ **.....(4)**
- CCL = $-\log_2 |\psi R|$ ……(5)

CONCLUSION

The MIMO antenna, which spans frequencies such as 1.8GHz (GSM), 2.5GHz (WLAN), 3.3GHz (5G IoT), and 3.1-10.6GHz (UWB applications), is composed of two ultrawideband and four narrowband radiators as per theoretical design. For better results, less isolation, and improved performance, the antenna was constructed with a shared ground for real-time testing. A NodeMCU for Wi-Fi, an IoT gateway, and a GSM module were used in the performance evaluation. A thorough examination and validation of the antenna's effectiveness over a range of frequency bands and applications was made possible by the traditional methods used to get the results and convert them into diagrams using Origin and MS Excel.

REALISTIC CONSTRAINTS:

- The project does not discuss the impact of environmental factors, such as the presence of obstacles, on the antenna's performance.
- The project does not provide experimental results for the antenna's performance in non-ideal conditions, such as noisy environments.

ETHICAL BINDING:

- **Safety:** Ensure that the antenna design complies with safety standards to prevent any harm to users or the environment. This includes considerations for electromagnetic radiation exposure limits.
- **Fairness:** Consider the potential societal impacts of the antenna design, including its deployment and distribution. Aim to design a system that promotes fairness and equity in access and use.
- **Accessibility:** The design should aim to be accessible to all potential users, considering factors such as cost, ease of installation, and compatibility with various IoT devices.

FUTURE SCOPE

Multiband MIMO (Multiple Input Multiple Output) antennas have a bright future, thanks to the increased demand for high-speed data transmission, notably in wireless communication systems such as 5G and beyond. Here are some possible future applications for multiband MIMO antennas:

5G and Beyond: As 5G networks develop globally and become more powerful, the demand for multiband MIMO antennas will grow.

IoT and Smart Devices: The development of IoT and smart devices will increase the demand for multiband MIMO antennas that can support many frequency bands at once.

Satellite communication: Satellite communication systems can benefit greatly from multiband MIMO antennas, which allow for effective data transfer between satellites and ground stations.

Automotive Communication: As vehicles become more connected and autonomous, multiband MIMO antennas will be required to provide high-speed communication between vehicles, infrastructure, and other connected devices. These antennas can increase the reliability of vehicle-to-vehicle (V2V) and vehicle-to-infrastructure (V2I) communication systems, thereby improving road safety and traffic efficiency.

mmWave Communication: Multiband MIMO antennas can enable communication in millimeter-wave (mmWave) frequency bands, which provide much higher data speeds but less range than typical microwave frequencies.

REFERENCES

1. Kumar, Pawan, Shabana Urooj, and Areej Malibari. "Design and implementation of quad-element super-wideband MIMO antenna for IoT applications." IEEE Access 8 (2020): 226697-226704.
2. Thiruvenkadam, Saminathan, et al. "Design and performance analysis of a compact planar MIMO antenna for IoT applications." Sensors 21.23 (2021): 7909.
3. Jhamb, K., L. Li, and K. Rambabu. "Frequency adjustable microstrip annular ring patch antenna with multi-band characteristics." IET microwaves, antennas & propagation 5.12 (2011): 1471-1478.
4. Li, Daotie, and Jun-Fa Mao. "Koch-like sided Sierpinski gasket multifractal dipole antenna." Progress in Electromagnetics research 126 (2012): 399-427.
5. Deshmukh, Amit A., and K. P. Ray. "Compact broadband slotted rectangular microstrip antenna." IEEE antennas and wireless propagation letters 8 (2009): 1410-1413.
6. Yan, Zhengzheng, et al. "Multi-omics analyses of airway host–microbe interactions in chronic obstructive pulmonary disease identify potential therapeutic interventions." Nature Microbiology 7.9 (2022): 1361-1375.
   Sharma, Sameer Kumar, et al. "Triple-band metamaterial-inspired antenna using FDTD technique for WLAN/WiMAX applications." International Journal of RF and Microwave Computer-Aided Engineering 25.8 (2015): 688-695.
7. Gupta, R.K.; Kumar, G. Printed dual band monopole antenna structures for WLAN applications. Microw. Opt. Technol. Lett. 2008, 50, 2483–2487.
8. Dehmas, M., et al. "Compact dual band slotted triangular monopole antenna for RFID applications." Microwave and Optical Technology Letters 60.2 (2018): 432-436.
9. Gyasi, K.O.; Wen, G.; Inserra, D.; Huang, Y.; Li, J.; Ampoma, A.E.; Zhang, H. A compact broadband cross-shaped circularly polarized planar monopole antenna with a ground plane extension. IEEE Antennas Wirel. Propag. Lett. 2018, 17, 335–338.
10. . Chaturvedi, Divya, Arvind Kumar, and Ayman A. Althuwayb. "A dual-band dual-polarized SIW cavity-backed antenna-duplexer for off-body communication." Alexandria Engineering Journal 64 (2023): 419-426.
11. Aw Awais, Qasim, et al. "A novel dual ultrawideband CPW-fed printed antenna for Internet of Things (IoT) applications." Wireless Communications and Mobile Computing 2018 (2018).

APPENDIX

GSM:

Figure a: GSM

GSM (Global System for Mobile Communications) modules are essential components of cellular communication devices, allowing voice and data transmission across GSM networks. Despite the introduction of newer technologies such as 4G and 5G, GSM continues to play an important role, particularly in applications that require reliable and extensive cellular service. GSM modules are commonly used in IoT (Internet of Things) and M2M (Machine-to-Machine) communication applications, where devices must communicate data over cellular networks without requiring high-speed data rates. These applications include remote monitoring, asset tracking, smart metering, and industrial automation.

USRP Transmitter:

Figure b: USRP Transmitter

A USRP (Universal Software Radio Peripheral) transmitter sends radio signals via software-defined radio (SDR) technology. USRP transmitters are extremely adaptable and programmable, making them ideal for a wide range of applications in wireless communication, research, and education.

MICROCONTROLLER:

Figure c: Microcontroller

Microcontrollers are the primary processing units in both MIMO systems and IoT applications, performing critical services such as signal processing, system control, data management, networking, and security. They enable the creation of advanced wireless communication networks and intelligent IoT devices that improve connectivity, efficiency, and functionality across multiple domains.